CHEMMEDCHEM

CHEMISTRY ENABLING DRUG DISCOVERY

Accepted Article

Title: Synthesis of CA4 carboxamides mimicking with sulfonyl piperazines by a molecular hybridization approach: In vitro cytotoxicity evaluation and tubulin polymerization inhibition.

Authors: Ahmed Kamal, Chetna Jadala, Manda Sathish, Anchi Pratibha, Ramya Tokala, Uppu Jaya Lakshmi, Velma Ganga Reddy, Nagula Shankaraiah, and Chandaraiah Godugu

To be cited as: *ChemMedChem* 10.1002/cmdc.201900541

Link to VoR: http://dx.doi.org/10.1002/cmdc.201900541

A Journal of

ChemPubSoc Europe

WILEY-VCH

www.chemmedchem.org

Synthesis of combretastatin-A4 carboxamides mimicking with sulfonyl piperazines by a molecular hybridization approach: *In vitro* cytotoxicity evaluation and tubulin polymerization inhibition

Chetna Jadala[a], Manda Sathish[b], Pratibha Anchi[c], Ramya Tokala[a], Uppu Jaya Lakshmi[a], Velma Ganga Reddy[b], Nagula Shankaraiah[a]*, Chandraiah Godugu[c]* and Ahmed Kamal[b,d]*

Abstract: Molecular hybridization approach is a promising structural modification tool to design new chemical entities (NCEs) by mimicking two different pharmacophoric units into one scaffold to enhance the biological properties. With this aim, combretastatin A4 acids were integrated with sulfonyl piperazine scaffolds as a one molecular platform and evaluated for their *in vitro* antiproliferative activity against a panel of human cancer lines cell lines namely, lung (A549), mouse melanoma (B16F10), breast (MDA MB-231, MCF-7) and colon (HCT-15) by MTT assay. Amongst which the compound *(E)-3-(4-Chlorophenyl)-1-(4-((4-chlorophenyl)sulfonyl)piperazin-1-yl)-2-(3,4,5-trimethoxyphenyl)prop-2-en-1-one (***5ab**) displayed significant IC_{50} values in the range of 0.36 to 7.08 μM against the selected cancer cell lines. Moreover, **5ab** was found to be the most potent member of this series with IC_{50} 0.36±0.02 μM. Further investigations revealed that the compound **5ab** displayed significant inhibition of tubulin assembly with IC_{50} 5.24±0.06 μM and molecular docking studies also disclosed the binding of **5ab** effectively at the colchicine binding site. The flow cytometric analysis demonstrated that the compound **5ab** caused cell cycle arrest at G2/M phase in A549 cells. Compound **5ab** induced apoptosis in A549 cells which was further evaluated by different staining assays such as DAPI and AO which undoubtedly speculated, the induction of apoptosis. To study the anti-migration with **5ab**, cell migration/scratch wound assay was performed and the extent of apoptosis was studied by Annexin-V, including mitochondrial potential by JC-1 staining.

Introduction

Microtubules are vital components of cytoskeleton composed of α, β-tubulin heterodimer assembly, majorly engaged in cell division which is responsible for spindle formation and separating duplicated chromosomes prior to cell division; this makes them as an imperative target for anticancer drugs[1]. In this breakthrough, both natural and synthetic derivatives are capable of targeting microtubules assembly or disassembly that has attracted much attention [2]. The typical paradigms that are acting as antimitotic agents are epothilone A [3], paclitaxel [4], vinblastine [5] and combretastatin A4 (Figure 1) [6], which are mainly categorized in the management of ovarian, prostate and breast cancers [7, 8]. Besides the efficacy and medical usefulness of presently available drugs, the main drawback is systemic toxicity and poor biopharmaceutical properties [9, 10]. As a result, the search for novel antimicrotubule scaffolds with improved pharmacodynamic profile with lower toxicity is the main spotlight for many researchers.[11] Tubulin has three binding sites, the taxane binding site, vinca binding site and the colchicine binding site [12, 13]. Molecules that act as microtubule stabilizing agents prevent depolymerisation by targeting the taxane binding site [14, 15]. While the agents which inhibit α, β-tubulin assembly towards polymerization, target the vinca and colchicine binding sites [16]. The ligands interacting at colchicine binding site were extensively studied and many other interesting compounds such as podophyllotoxin, colchicine and CA4 were identified. To that end, CA4 was isolated from *Combretum caffrum* [17] has imperative pharmacological profile, structural simplicity and potent antitumor properties. The *cis*-configuration of the double bond between the two aryl rings and the 3, 4, 5-trimethoxy system on the A ring are essential requirements for its biological activity [18-20], however it suffers from lower water solubility and readily isomerization of double bond to inactive *trans* form [21, 22]. It is evident from the previous reports that diverse ligands mimicking CA4 were designed and explored their structure activity relationships and chemical modifications and were evaluated for their anti-proliferative activities. C. Borrel *et al.* have prepared two series of compounds bearing substituent either a carboxamide or a carbamate group, on C1 position of the olefin bridge adjacent to the A-ring of these compounds, carboxamide substitution was less cytotoxic but displayed increased antitubulin activity (Figure 1, CA4 carboxamide) [23, 24]. Therefore, the above findings inspired us to design CA4 ligands having amide linkage by different motifs with the goal of including a new profile or a novel set of molecules with improved cytotoxicity and lower toxicity profile.

On the other hand, a theme has been gaining importance in cancer chemotherapy by the use of combinations of two or more agents [25]. With respect to molecular hybridization approach, two important fragments are merged which could be beneficial for the treatment of cancer, considering the fact that the

[a] *C. Jadala, R. Tokala, U.J. Lakshmi, Dr. N. Shankaraiah*
Department of Medicinal Chemistry
National Institute of Pharmaceutical Education and Research (NIPER),
Hyderabad, 500037, India.
E-mail: shankar@niperhyd.ac.in
[b] *M. Sathish, V.G. Reddy, Dr. Ahmed Kamal*
Medicinal Chemistry and Pharmacology,
CSIR-Indian Institute of Chemical Technology,
Hyderabad, 500007, India.
Email: ahmedkamal@iict.res.in
[c] *P. Anchi, C. Godugu*
Department of Regulatory Toxicology,
National Institute of Pharmaceutical Education and Research (NIPER),
Hyderabad, 500037, India.
Email: chandra.niperhyd@gov.in
[d] *Dr. Ahmed Kamal*
School of Pharmaceutical Education and Research (SPER) Jamia Hamdard,
New Delhi, 110062, India.
Email: ahmedkamal@iict.res.in
Supporting information for this article is given via a link at the end of the document.

sulfonamide and piperazine derivatives represent a class of pharmacologically proficient scaffolds having diverse biological activities. Sulfonamides were extensively used owing to their clinical usage as anti-inflammatory [26], anticancer [27, 28], antimicrobial [29, 30], antiviral and HIV protease inhibitors [31]. Earlier reports have shown significant insights and used in clinical studies about the effective antitumor activity of novel sulfonamide derivatives and several colchicine binding site agents bearing the sulfonamide group, such as J30 [32] and T138067 [33] (Figure 1). Furthermore, in recent years the piperazine derivatives were also reported to be diverse structural motifs and procured much attention due to their versatile properties [34-36]. It has been found that *N*-substituted piperazine compounds possess a wide range of pharmaceutical activities, such as anticancer [37], antifungal [38] and antimicrobial [39] activities. Piperazine and its derivatives are one of the important scaffolds, besides having potent antibacterial activity such as piperazinyl-linked ciprofloxacin dimers [40], also possess anticancer activity. Plinabulin which is a piperazine derivative with colchicine-like tubulin depolymerization activity displayed IC_{50} values at nanomolar scale [41]. Inspired by the biological profile and synthetic accessibility of combretastatin A-4 and sulfonyl piperazine and our continued interest in developing novel anticancer agents led to molecular hybridization [42] of these molecules shown in Figure 1. In this perspective, a series of novel compounds were synthesized and evaluated for their *in vitro* anticancer activity and the most promising compound was also further evaluated for its *in vitro* cytotoxicity.

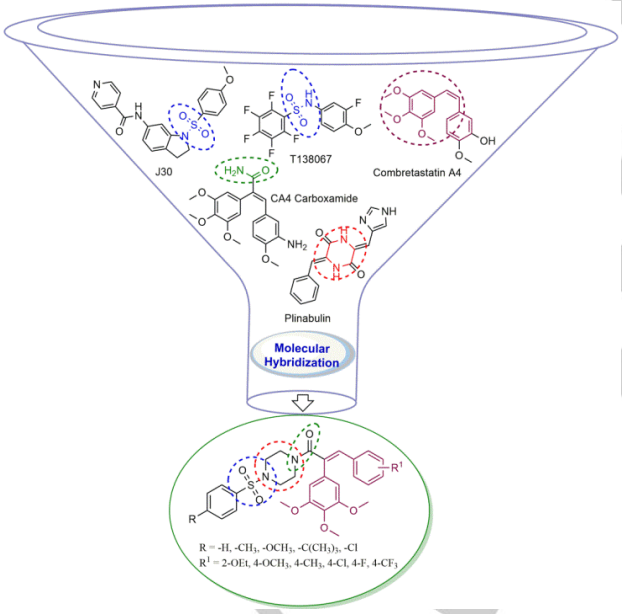

Figure 1. Chemical structures of novel tubulin inhibitors and molecular hybridization approach to combretastatin A-4 inspired sulfonyl piperazine scaffolds **5a–ad**.

Results and Discussion

Chemistry

The synthetic route for the preparation of desired combretastatin CA-4-linked sulfonyl piperazine hybrids **5a–ad** was outlined in Scheme 1. We began with the synthesis of different substituted sulfonamides **2a–e** by reacting piperazine with different benzenesulfonyl chlorides **1** in CH_2Cl_2 as solvent. Next, phenyl acetic acid (**3**) was treated with substituted aldehydes to afford the (*E*)-3-phenyl-2-(2,3,4-trimethoxyphenyl)acrylic acids **4a–f**. Then the desired combretastatin CA-4-linked sulfonyl piperazine hybrids **5a–ad** were successfully synthesized by acid amine coupling between the intermediates **2a–e** and **4a–f** using EDCI and HOBt in dry DMF. The corresponding crude compounds were purified *via* column chromatography and obtained with good to excellent yields (85-90%). All the final compounds **5a–ad** were unambiguously characterized by spectroscopic studies (^{1}H NMR, ^{13}C NMR and HRMS). The ^{1}H NMR spectrum of **5a** showed a significant broad peak of 4 protons of piperazine from *δ* 2.7-3.0 ppm and another four protons were observed at *δ* 3.68 ppm and a prominent *cis* proton appeared at *δ* 6.62 ppm and rest of the aromatic protons appeared in the range of *δ* 7.9–6.0 ppm.

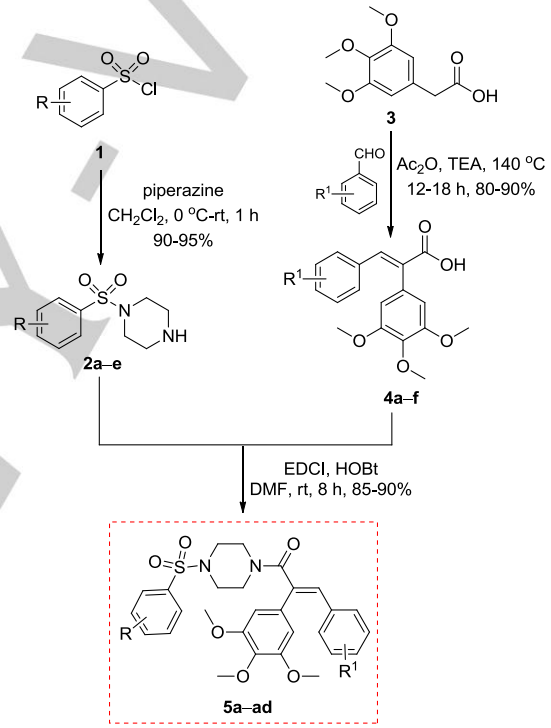

5a: R = H, R^1 = 2-OC_2H_5
5b: R = H, R^1 = 4-OMe
5c: R = H, R^1 = 4-CH_3
5d: R = H, R^1 = 4-Cl
5e: R = H, R^1 = 4-F
5f: R = H, R^1 = 4-CF_3
5g: R = CH_3, R^1 = 2-OC_2H_5
5h: R = CH_3, R^1 = 4-OMe
5i: R = CH_3, R^1 = 4-CH_3
5j: R = CH_3, R^1 = 4-Cl
5k: R = CH_3, R^1 = 4-F
5l: R = CH_3, R^1 = 4-CF_3
5m: R = OCH_3, R^1 = 2-OC_2H_5
5n: R = OCH_3, R^1 = 4-OMe
5o: R = OCH_3, R^1 = 4-CH_3
5p: R = OCH_3, R^1 = 4-Cl
5q: R = OCH_3, R^1 = 4-F
5r: R = OCH_3, R^1 = 4-CF_3
5s: R = 3°-C_4H_9, R^1 = 2-OC_2H_5
5t: R = 3°-C_4H_9, R^1 = 4-OMe
5u: R = 3°-C_4H_9, R^1 = 4-CH_3
5v: R = 3°-C_4H_9, R^1 = 4-Cl
5w: R = 3°-C_4H_9, R^1 = 4-F
5x: R = 3°-C_4H_9, R^1 = 4-CF_3
5y: R = Cl, R^1 = 2-OC_2H_5
5z: R = Cl, R^1 = 4-OMe
5aa: R = Cl, R^1 = 4-CH_3
5ab: R =Cl, R^1 = 4-Cl
5ac: R = Cl, R^1 = 4-F
5ad: R = Cl, R^1 = 4-CF_3

Scheme 1. Synthesis of combretastatin A-4 linked sulfonyl piperazine hybrids **5a–ad**.

In the ^{13}C NMR spectrum of **5a**, the carbonyl and methyl carbons appeared at *δ* 170.0 and 15.4 ppm, respectively. methoxy carbons obtained at 56.0 and 60.0 ppm and remaining aromatic carbons appeared in the range of *δ* 156.5–105.8 ppm. Similarly, all the remaining compounds ^{1}H and ^{13}C NMR spectra were noticed in the similar pattern. The HRMS (ESI) of **5a–ad** showed characteristic $[M + H]^{+\cdot}$ peaks equivalent to their molecular formulae.

Biology

Antiproliferative activity

The newly synthesized hybrids **5a–ad** were evaluated for their *invitro* antiproliferative potency against selected human cancer cell lines such as lung (A549), mouse melanoma (B16F10) breast (MDA-MB-231, MCF-7) and colon (HCT-15) by the aid of 3-(4,5-dimethylthiazol-2-yl)-2,5-diphenyltetrazolium bromide (MTT) assay [43]. The results of respective cytotoxicity data were displayed in the form of IC_{50} (concentration required to inhibit 50% of the cancer cells), along with combretastatin A4 IC_{50} which was included as the standard (Table 1). From the results, it can be inferred that compounds **5d**, **5f**, **5h**, **5j**, **5t**, **5u**, **5ab**, **5ac** and **5ad** exhibited significant cytotoxicity in almost all the cancer cell lines with IC_{50} values ranging from 0.43±0.06 to 29.72±4.53 μM. Amongst all the compounds tested, **5ab** exhibited remarkable cytotoxicity in all the cancerous cell lines displaying IC_{50} ranging from 0.36±0.02 μM to 7.05±3.36 μM.

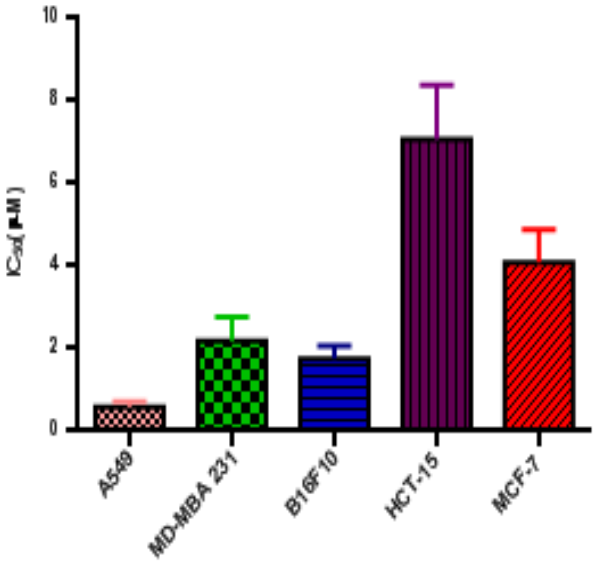

Figure 2. Cytospecificity of compound **5ab** towards different cell lines. IC_{50} values were calculated after 48 h treatment with compound **5ab** Values are represented by mean ± SEM of three independent experiments.

Moreover, the compound **5ab** is active as much as CA4 showing IC_{50} value as 0.36±0.02 μM whereas CA4 exhibited IC_{50} of 0.43±0.16 μM on A549 cell line and it was noteworthy that the compound **5ab** was comparitively less potent for the other studied cell line showing IC_{50} 7.05±3.36 μM on HCT cell line.

From the close analysis of Table 1, the structure activity relationship (SARs) for these compounds has been constructed by considering the sulfonamide ring was selected, which is diversified with 5 substituents of which 4-chloro substitution on C4 of sulfonamide phenyl ring has shown potent activity as in case of **5z**, **5aa** and **5ab** of which the compound **5ab** was most potent. The other substituents on sulfonamide ring such as H, methyl, methoxy and tertiary butyl were comparatively less active than 4-chloro substitution. From this, we could speculate that 4-chloro substitution on C4 of sulfonamide ring was responsible for the compound to show cytotoxicity. It was also noteworthy to consider the varaiable groups on CA4 ring for eg., the compounds **5z** and **5aa** having 4-chloro substitution at C4 of CA4 B-ring were moderately active towards the tumor cell lines investigated but the other compounds such as **5p** and **5v** with chloro substitution on C4 of CA4 ring were comparatively less active. Furthermore, the compounds such as **5a**, **5g**, **5m**, **5s** and **5y** with ethoxy substitution on C4 of CA4 B-ring were less potent on all the cell lines investigated. Finally, keeping in view of above speculations, we have arranged the compounds in order of their cytotoxicity based on substitution on sulfonamide and CA4 ring as Cl-Cl>Cl-Me>Cl-OMe. To find out the selectivity towards cancer cells, the most active compound **5ab** was tested on normal human keratinocyte cell line (HaCaT). Interestingly, compound **5ab** was found to be almost 3 times more selective on A549 cells compared to normal HaCaT cells. The promising cytotoxicity of compound **5ab** on A549 cells provoked us to explore for its effect at cellular level.

Cell Migration/Scratch Wound assay

Cancerous cells multiply and migrate throughout the body, with the help of extracellular matrix by intravasing into blood circulation, subsequently attaching to a distant site, and finally extravasing by making its own identity. This invasion is currently considered as a main reason for death in cancer patients termed as metastatic progression [44]. Hence, to evaluate this property by the potent hybrid **5ab** on A549 cancer cells, the assay was performed by cell culture wound closure assay. It can be observed from Figure 3 that after 24 h the wound area is filled with 17.40±4.03% of untreated control cells, while the treatment with compound **5ab** in 0.1 μM and 0.25 μM concentration depicted significant inhibition of cell migration with 10.48±6.43%, 5.55±1.83% cells respectively in the wounded area. While in 0.5 μM and CA4 there was no migration observed. From the above findings, it can be scrutinized that the compound inhibited cell migration in a dose dependent manner.

Apoptosis detection studies

The human cancerous cell have the capability to escape the apoptosis or programmed cell death for cell survival and contribute for the tumor progression, invasion and drug resistance; therefore most of the anticancer drugs strive for regenerating apoptosis in the cancer cells which is now considered as an attractive strategy in cancer therapy. Therefore, we considered to evaluate the apoptosis inducing effect of compound **5ab** on A549 cell lines using CA4 as a positive control by using staining studies such as AO, DAPI, Annexin-V propidium and JC-1 assay.

Table 1. IC_{50} (μM *In vitro* cytotoxic activity (IC_{50} in μM)[a] of combretastatin A4 linked sulfonyl piperazine hybrids **5a–ad**

Compound	A549[b]	B16F10[c]	MDA MB-231[d]	HCT-15[e]	MCF-7[f]	HaCaT[g]
5a	>30	>30	>30	>30	>30	-
5b	>30	>30	>30	>30	>30	-
5c	>30	>30	>30	>30	18.20±1.37	-
5d	15.46±4.17	7.50±0.85	17.43±1.25	>30	29.72±4.53	-
5e	>30	>30	>30	>30	>30	-
5f	24.71±0.51	11.108±0.37	5.49±0.65	>30	3.70±0.81	-
5g	>30	>30	>30	>30	>30	-
5h	6.38±2.77	4.11±0.96	1.83±0.47	>30	>30	-
5i	>30	>30	>30	>30	>30	-
5j	15.93±2.81	7.36±1.51	6.46±1.17	3.27±2.13	24.68±5.16	-
5k	>30	>30	>30	>30	>30	-
5l	6.38±2.77	3.96±1.29	14.33±2.45	>30	2.23±0.23	-
5m	>30	>30	>30	>30	>30	-
5n	>30	>30	>30	>30	18.94±1.822	-
5o	>30	>30	6.36±0.78	3.25±0.80	>30	-
5p	>30	>30	>30	>30	>30	-
5q	>30	>30	>30	>30	>30	-
5r	>30	>30	>30	>30	>30	-
5s	>30	>30	>30	>30	>30	-
5t	8.44±0.80	1.01±0.07	4.20±1.08	17.07±1.32	18.87±0.85	-
5u	18.16±1.04	>30	4.50±0.27	4.10±0.95	>30	-
5v	>30	>30	>30	>30	>30	-
5w	>30	>30	>30	>30	>30	-
5x	>30	>30	>30	>30	>30	-
5y	>30	>30	>30	>30	>30	-
5z	2.66±0.26	5.42±3.83	2.23±0.14	>30	0.78±0.06	-
5aa	0.72±0.20	2.14±0.16	2.52±1.19	6.20±2.19	>30	-
5ab	0.36±0.02	1.75±0.44	2.16±0.83	7.05±3.36	4.08±1.10	0.92±0.01
5ac	>30	>30	>30	>30	>30	-
5ad	>30	>30	>30	>30	>30	-
CA-4 [h]	0.43±0.16	0.03±0.00	0.79±0.21	1.92±0.92	2.12±0.21	0.63±0.17

[a] 50% Inhibitory concentration after 48 h of drug treatment and the values are average of three individual experiments. [b] Human lung cancer cells, [c] Mouse Skin cancer cells, [d] Human Breast cancer cells [e] Human colon cancer cells, [f] Human Breast cancer cells, [g] Human keratinocyte, [h] Combretastatin A-4 = CA-4. All the values are expressed as Mean ± SEM in which each treatment was performed in triplicate wells.

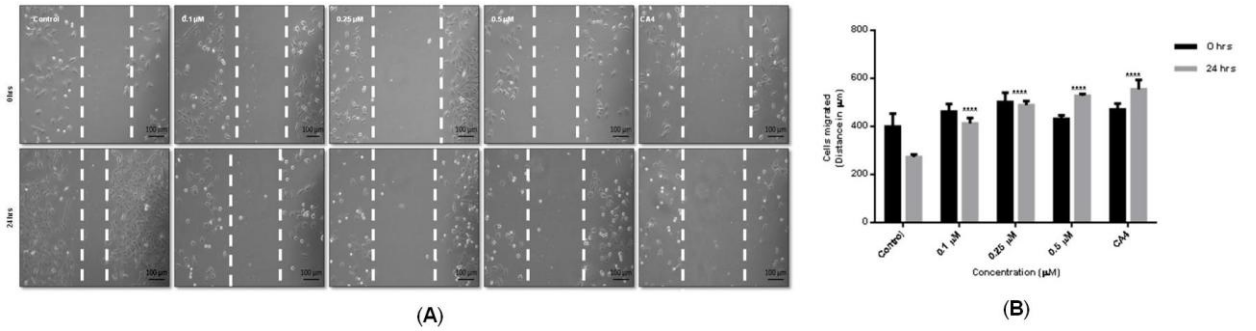

(A) (B)

Figure 3. (**A**) Images of scratch wound assay (at magnification 100X). After reaching near confluency, monolayer was scratched and treated with the compound **5ab** and **CA4** for 24 h. Respective images were taken at 0 and 24 h. (**B**) Represents % wound closure. Data presented were mean ±SEM of similar three independent experiments ****p<0.0001 versus control at 24 h

Phase contrast imaging

To examine whether the treatment with the compound **5ab** could lead to loss of cell viability and induce apoptosis, after 48 h of treatment with compound at variable concentrations (0.1, 0.25, 0.5 and CA4 (1 µM), the cells were observed for the morphological changes under phase contrast microscope.[45] From the Figure 4, it is evident that increasing the compound concentration has led to significant cell death in comparison to the positive control (CA4). Apart from viability, compounds induced apoptosis related morphological changes like cell blebbing and condensation of nucleus. This signifies that the compound **5ab** induced typical morphological changes in A549 lung cancer cells.

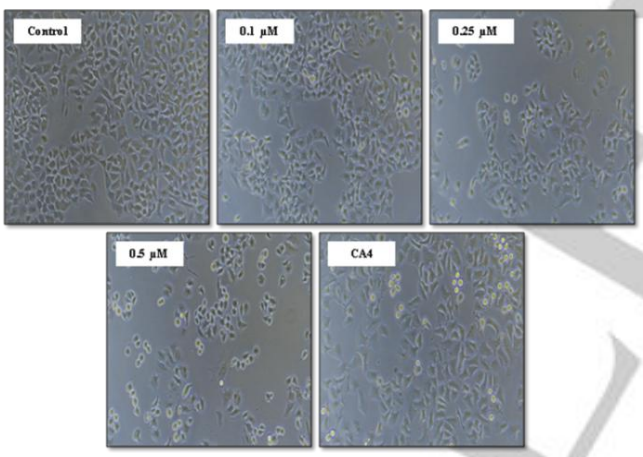

Figure 4. Phase contrast imaging of A549 cells after treatment with compound **5ab**.and CA-4. Images were taken after 48 h treatment and observed under phase contrast microscope at magnification of 200X.

Acridine orange staining

Acridine orange is a stain technique which enables to identify the apoptotic cells [46]. This assay demonstrates on the principle that acridine orange can penetrate the live cells by which they appear healthy with dark green color fluorescence. Herein, upon treatment of compound **5ab** and CA4, various apoptotic phase cells were identified by this staining. From the Figure 5, it depicts that at the lowest concentration of 0.1 µM, the cells have least apoptotic activity and with increasing the concentration we observed membrane blebbing, destructive fragmentation and irregular distribution of chromatin in analogous with CA4 as indicated in Figure 5.

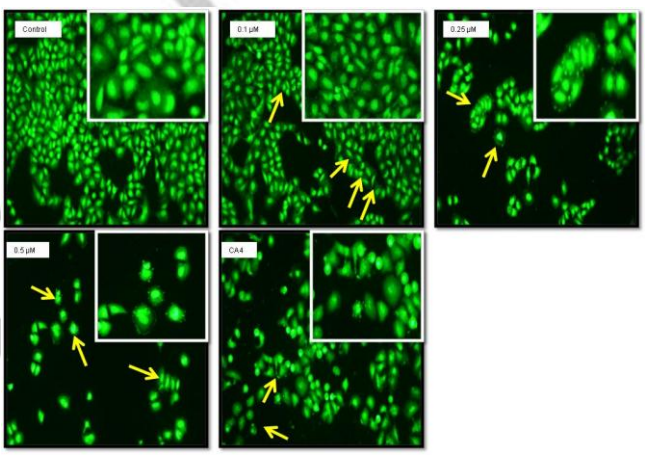

Figure 5. Representative images of AO staining in A549 cells. Cells were treated with compound **5ab** at concentrations of 0.1, 0.25, 0.5 µM and CA4 (1 µM) for 48 h. The images were captured with a fluorescence microscope at 200X magnification

DAPI staining assay

DAPI diffuses easily into disrupted cell membrane rather than intact cell membrane [47]. Therefore, stained cells showed less intensity than normal cells. From the results, it is clear that compound **5ab** in comparison to standard (CA4) induced massive nuclear damage with increasing concentration of treatment. It can be observed that a bright condensed and fragmented nucleus is identified by the DAPI staining and is a clear indication of apoptosis. Furthermore, margination of nucleus due to which horseshoe shaped structure was also observed as shown in Figure 6.

Annexin V/ PI dual binding assay

Various events are reported in cell changes during the apoptosis, which includes fragmentation of the nucleus, chromosomal DNA and chromatin condensation. Along with this externalization of phosphatidyl serine is also considered as one of the characteristic feature of cell undergoing apoptosis. Therefore to evaluate this, Annexin V-PI staining technique was performed on A549 cells with compound **5ab** at different concentrations (0.1,

0.25 and 0.5 μM), CA4 and compared with untreated cells for about 48 h. As shown in Figure 7, the compound **5ab** and CA4 caused increase in the percentage of apoptotic cells with 11.67%, 16.77%, 35.55%, and 16.88% respectively. This suggests that compound **5ab** inhibited cell proliferation by inducing apoptosis in A549 cells in a dose dependent manner.

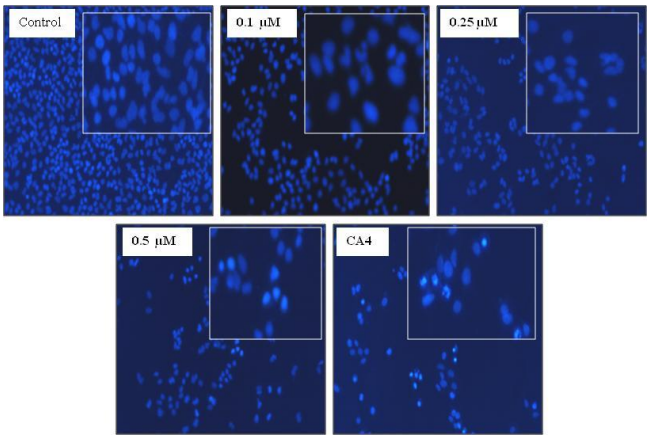

Figure 6. Representative images of DAPI staining in A549 cells. Cells were treated with compound **5ab** at concentrations of 0.1, 0.25, 0.5 μM and CA4 for 48 h. The images were captured with a fluorescence microscope at 200X magnification

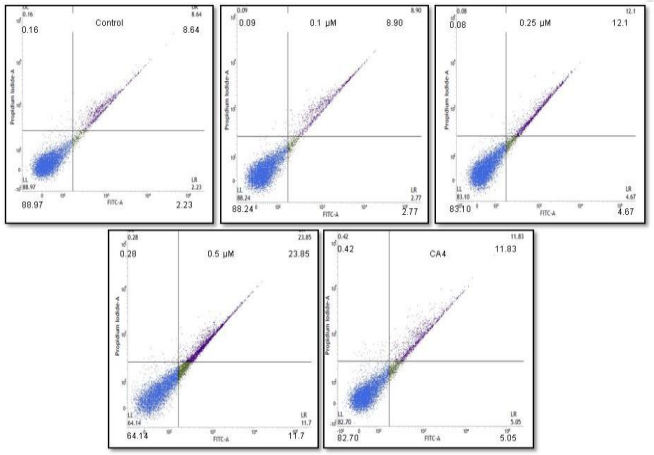

Figure 7. Cells were treated with 0.1, 0.25 and 0.5 μM concentration of compound **5ab** and CA4 for 48 h and stained with Annexin V and PI. Cells were then washed with PBS and dispersed in PBS until analysis by Flow cytometer (BD FACSVerse™, USA). 10,000 events were analyzed by the instruments.

Measurement of Mitochondrial Membrane Potential

Health of mitochondria is crucial for the normal physiology of cells by which it preserves the bioenergetics functions. This can be represented by means of mitochondrial membrane potential (mΨΔ). Alteration in this potential is an indication of early events that occur during the apoptotic process. To evaluate the health status of cancerous cells in terms of apoptosis upon treatment with compound **5ab**, tetraethylbenzimidazolylcarbocyanine iodide (JC-1) mΨΔ assay was performed [48]. This assay works on the principle that JC-1 a cationic dye binds dominantly to the J monomers formed during hyperpolarisation in the cells (generally occurs in ill stated cells/apoptotic cells) and emits fluorescence at 590±17.5 nm. However, normal healthy cells contain more J aggregates and less monomers due to which JC-1 dye couldn't bind and emits fluorescence at 530±15 nm. Flow cytometry analysis of A549 cells after treatment with compound **5ab** revealed that the compound has disrupted the mΨΔ in contrast to control cells. The mΨΔ is represented in terms of P1 (normal mΨΔ) and P2 (altered mΨΔ) populations in Figure 8. When total of 10,000 cells were analyzed for this assay, compound **5ab** increased the P2 (J monomers) population from 36.62 to 69.88% in comparison to control. Followed by this, on comparison with a positive control, the compound **5ab** at 0.25 μM, was found to be on par with the standard CA-4.

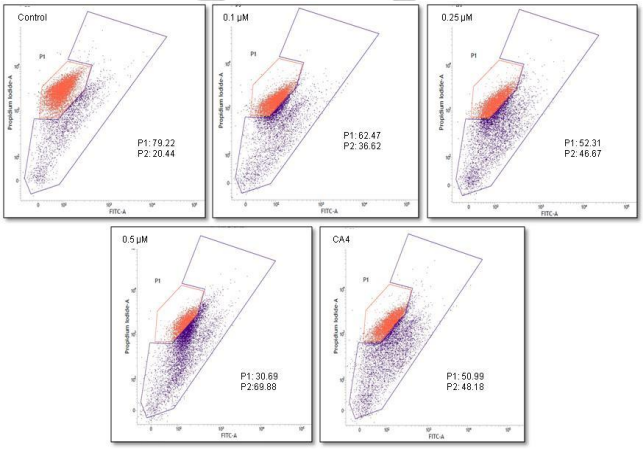

Figure 8. Image representing ratio of J aggregates (P1-red colour) to J monomers (P2-purple colour). Fluorescence of JC-1 was analyzed using Flow cytometer (BD FACSVerse™, USA). Here 10,000 events were calculated for the analysis.

Cell cycle analysis

To further study whether the compound **5ab** could arrest the process of mitosis, cell cycle distribution of A549 cells was assessed using well studied PI staining procedure. The cells were treated with different concentrations (0.5 and 1 μM) of compound **5ab** for 24 h, after which cell cycle distribution was analyzed through flow cytometry [49]. The results revealed that the treatment with compound **5ab** resulted with significant accumulation of A549 cells in G2/M phase from 25.44% to 65.44% when compared with control in a dose dependent manner. From the Figure 9, it can be inferred that the compound **5ab** arrested the lung cancer cells in G2/M phase.

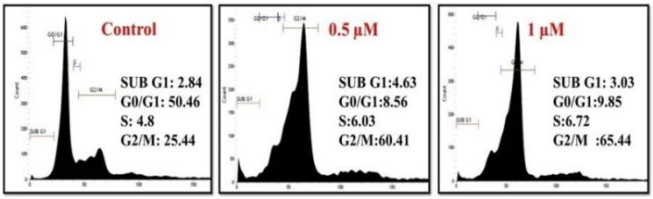

Figure 9. Effect of compound **5ab** on the progression of cell cycle in A549 cells treated at concentrations of 0.5 and 1 μM and compared with control. After 24 h of treatment time, the cells cycle profile was performed by using propidium iodide staining method and analyzed by Flow cytometry analysis (BD FACSVerse™, USA analysis). The percentages of G1, S and G2/M phase cells were calculated from the DNA content histograms.

Tubulin polymerization inhibition

The antimitotic effect of combretastatin A4 is due to inhibition of the function of microtubules. CA-4 binds to tubulin at the colchicine binding site. It binds to tubulin heterodimer leads to disruption and consequently causing inhibition of its polymerization into microtubules. This further causes formation of irregular mitotic spindles and metaphase arrest of mitotic cells. Colchicine is known to be toxic and has few therapeutic uses but the binding of CA-4 to the colchicine site of tubulin has shown potent cytotoxicity against cancer cells [50]. Furthermore, the newly synthesized scaffolds mimics the CA-4 structurally, in this context, to investigate the correlation between cytotoxicity of these compounds and tubulin, compound **5ab** was examined for its effect on tubulin polymerization in a cell-free *in vitro* assay [51], Paclitaxel and CA-4 were chosen as positive control where Paclitaxel being the tubulin enhancer and CA-4 as tubulin inhibitor. Tubulin polymerization was monitored by the increase in fluorescence at 360 nm (excitation) and 440 nm (emission) for 1 h at 37 ^{o}C. The compounds were included at a final concentration of 1.25, 2.5, 5.0 and 10.0 µM respectively. The experiment was performed in duplicates. The % inhibition of Compound **5ab** screened at 10 µM was found to be 50%. As illustrated in Figure 10, **5ab** efficiently inhibited tubulin polymerization in a dose-dependent manner with IC_{50} value of 5.24±0.06 µM.

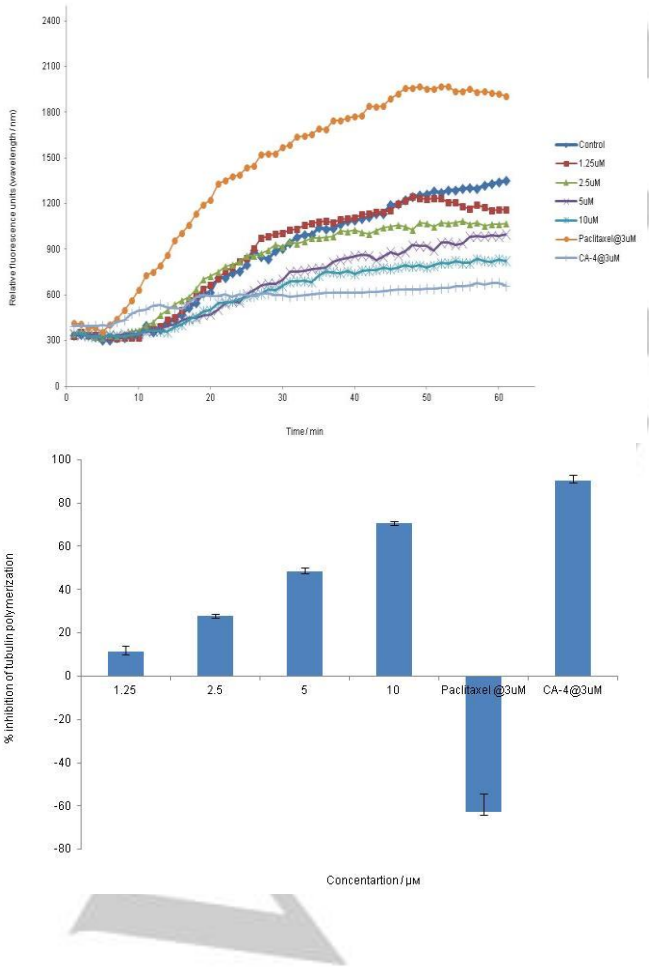

Figure 10. Effect of compound **5ab** on tubulin polymerization inhibition. Data presented were mean ±SEM of three similar independent experiments.

Molecular docking study

To further reveal the mode of binding with the tubulin, the potent compound **5ab** was docked into the combretastatin-binding site of tubulin protein (PDB ID: 5LYJ) [52] located at the interface of α, β-subunits. Molecular docking studies were performed by using GLIDE docking module of Schrödinger suite 2017-1[53]. The best docked pose of ligand **5ab** was well accommodated in the combretastatin binding pocket between α,β-subunits and has been represented in Figure 11 (**A**). The most active compound **5ab** exhibited two strong hydrogen-bonding interactions with the active residues. The 4-methoxy phenyl of **5ab** displayed hydrogen bond interactions with the hydroxyl group of Tyr202 (C-O…H-O) and the carbonyl oxygen and piperazine entity displays hydrogen-bonding with amine of Asp251 (C-O…H-N) as represented in Figure 11 (**B**). The piperazine moiety acts as linker that holds the sulfonyl phenyl moiety towards α-chain of the active pocket. Further, several hydrophobic interactions were observed for the piperazine and sulfonyl phenyl of ligand **5ab** with amino acid residues of α-chain Ala 180, Val 181 and β-chain residues such as Leu248, Ala250, Leu252, Leu255, and Met259. The combretastatin moiety of the compound **5ab** extend into the active pocket on β-chain and is surrounded by Tyr202, Phe169, Val238, Cys241, Leu242, Phe268, Val315, Ala316, Ala317, Ile318, Phe377 and Ile378 amino acid residues. The superimposition of the co-crystallized ligand and active ligand **5ab** was further established for the correlation of docking study with the *in vitro* tubulin assay and has been represented in Figure 11 (**C**). From the results, it was observed that the hydroxy phenyl group of co-crystal was superimposed with the sulfonyl phenyl of the ligand **5ab** and the *cis* oriented double bond of co-crystal gets superimposed with the amide bond of piperazine linker. However, the ligand **5ab** was well accommodated in the active pocket with good hydrogen bonds and numerous hydrophobic interactions with different amino acid residues, yet there lies a slight deviation by lacking the hydrogen bond interaction with Thr179 residue, which was actually observed in the co-crystal, which therefore, accounts for the weak inhibition of tubulin polymerization than CA4.

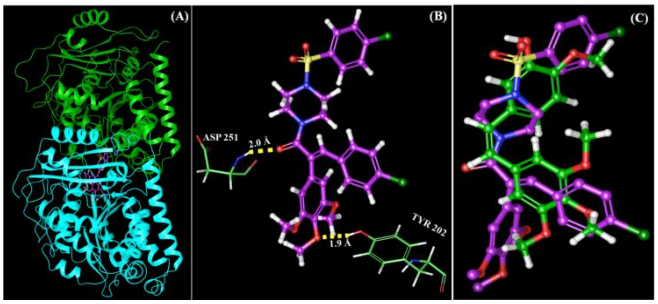

Figure 11. A) Compound **5ab** docked into the interface between α,β-subunits of tubulin protein (PDB ID: 5LYJ). Green color: α-subunit, Cyan color: β-subunit, Ligand is represented in magenta with ball and stick model. **B**) Hydrogen bond interactions of the ligand **5ab** with amino acid residues Tyr202 and Asp251; Ligand is represented in magenta and hydrogen bond interactions are denoted in yellow color. **C**) Superimposition of co-crystallized ligand (green) and best docked pose of ligand **5ab** (magenta) in the combretastatin binding site of α/β-tubulin interface (PDB ID: 5LYJ).

Conclusion

In conclusion, we have synthesized a series of new combretastatin A-4 linked sulfonyl piperazine hybrids **5a–ad** and further evaluated for their *in vitro* antiproliferative activity on a panel of human cancer cell lines. This *in vitro* screening outcome signifies that the most active compound **5ab** displayed extensive range of activity on all the tested cancer cell lines with IC_{50} value of 0.36±0.02 μM on A549 cells. The flow cytometric analysis indicated the cell cycle arrest in A549 cells at G2/M phase. In addition, the compound **5ab** efficiently inhibited tubulin polymerization with IC_{50} value of 5.24±0.06 μM and *in silico* studies also declared that the compound **5ab** binds at the colchicine binding site of the tubulin. Furthermore, the compound **5ab** showed apoptotic changes by decreasing the viable cells as in case of AO and DAPI staining assays. The other studies such as JC-1, Annexin-V, cell migration/scratch wound assay and phase contrast imaging, the compound **5ab** revealed the dose dependant inhibition by inducing apoptosis and mitochondrial damage that gave insights about cell migration and cell viability. Finally, the new series of compounds are potent to be proceeded as microtubule targeting cytotoxic agents in treating cancer.

Supporting information

Synthetic procedures, experimental details, spectral information (^{1}H and ^{13}C spectra) and biological evaluation are found in the supporting information of this article.

Acknowledgments

C. J., and R. T., are thankful to DoP, Ministry of Chemicals & Fertilizers, Govt. of India, New Delhi, for the award of NIPER fellowship. Dr. N. Shankaraiah is thankful to SERB, DST, Govt. of India for the start-up grant (YSS-2015-001709).

Conflict of interest

The authors declare no conflict of interest.

Keywords Combretastatin A-4 • sulfonyl piperazine • tubulin assembly • cell migration/scratch wound assay • cytotoxicity.

References

[1] a) A. Jordan, L. Wilson, *Nat. Rev. Cancer* **2004**, *4*, 253–265; b) R. Stephens and K. Edds, *Phys. Rev.* **1976**, *56*, 709–777.

[2] B. A. Teicher, *Clin. Cancer Res.* **2008**, *14*, 1610–1617.

[3] M. Trivedi, I. Budihardjo, K. Loureiro, T. R. Reid, J. D. Ma, *Future Oncol.* **2008**, *4*, 483–500.

[4] C. M. Spencer, D. Faulds, *Drugs* **1994**, *48*, 794–847.

[5] H. M. Robinson, *Biochem. Cell Biol.* **1991**, *69*, 581–582.

[6] J. Griggs, J. C. Metcalfe, R. Hesketh, *Lancet Oncol.* **2001**, *2*, 82–87.

[7] E. K. Rowinsky, R. C. Donehower, *Pharmacol. Ther.* **1991**, *52*, 35–84.

[8] G. Attard, A. Greystoke, S. Kaye, J. De Bono, *Pathol. Biol.* **2006**, *54*, 72–84.

[9] P. M. Checchi, J. H. Nettles, J. Zhou, J. P. Snyder, H. C. Joshi, *Trends Pharmacol.Sci.* **2003**, *24*, 361–365.

[10] M. Sridhare, M. J. Macapinlac, S. Goel, D. Verdier-Pinard, T. Fojo, M. Rothenberg, D. Colevas, *Anti-Cancer Drugs* **2004**, *15*, 553–555.

[11] M. N. Islam, Y. Song, M. N. Iskander, *J. Mol. Graphics Modell.* **2003**, *21*, 263–272.

[12] E. Nogales, M. Whittaker, R. A. Milligan and K. H. Downing, *Cell* **1999**, *96*, 79–88.

[13] R. B. Ravelli, B. Gigant, P. A. Curmi, I. Jourdain, S. Lachkar, A. Sobel, M. Knossow, *Nature*, **2004**, *428*, 198–202.

[14] S. B. Horwitz, *Trends Pharmacol. Sci.* **1992**, *13*, 134–136.

[15] J. J. Manfredi and S. B. Horwitz, *Pharmacol. Ther*. **1984**, *25*, 83–125.

[16] M. Jordan, *Curr. Med. Chem. Anti-Cancer Agents*, **2002**, *2*, 1–17.

[17] G. R. Pettit, S. B. Singh, E. Hamel, C. M. Lin, D. S. Alberts, D. Garcia-Kendal, *Experientia*, **1989**, *45*, 209–211.

[18] a) A. Brancale, R. Silvestri, *Med. Res. Rev.* **2007**, *27*, 209-238; b) A. Chaudhary, S. N. Pandeya, P. Kumar, P. P. Sharma, S. Gupta, N. Soni, K. K. Verma, G. Bhardwaj, *Mini-Rev. Med. Chem.* **2007**, *7*, 1186-1205.

[19] D. J. Chaplin, G. R. Pettit, S. A. Hill, *Anticancer Res.* **1999**, *19*, 189–195.

[20] J. W. Lippert III, *Bioorg. Med. Chem.* **2007**, *15*, 605–615.

[21] G. J. Rustin, S. M. Galbraith, H. Anderson, M. Stratford, L. K. Folkes, L. Sena, L. Gumbrell, P. M. Price, *J. Clin. Oncol.* **2003**, *21*, 2815–2822

[22] G. C. Tron, F. Pagliai, G. E. Del, A. A. Genazzani, G. Sorba, *J. Med. Chem.* **2005**, *48*, 3260-3268.

[23] K. Ohsumi, R. Nakagawa, Y. Fukuda, T. Hatanaka, Y. Morinaga, Y. Nihei, K. Ohishi, Y. Suga, Y. Akiyama, T. Tsuji, *J. Med. Chem.* **1998**, *41*, 3022-3032

[24] a) E. T. Haar, H. S. Rosenkranz, E. Hamel, B. W. Day, *Bioorg. Med.Chem.* **1996**, *4*, 1659-1671; b) C. Borrel, S. Thoret, X. Cachet, D. Guenard, F. Tillequin, *et al*, *Bioorg. Med. Chem.* **2005**, *13*, 3853–3864.

[25] V. T. DeVita, E. Chu, *Cancer Res.* **2008**, *68 (21)*, 8643-8653.

[26] R. F. Borne, R. L. Peden, I. W. Waters, M. Weiner, R. Jordan, *et al*., *J Pharm Sci*. **1974**, *63,* 615-617.

[27] J. Mun, A. A. Jabbar, N. S. Devi, S. Yin, Y. Wang, *et al*., *J. Med. Chem.* **2012**, *55*, 6738-6750.

[28] N. S. El-Sayed, E. R. El-Bendary, S. M. El-Ashry, M. M. El-Kerdawy, *Eur. J. Med. Chem.* **2011**, *46*, 3714-3720.

[29] Y. Genc, R. Ozkanca, Y. Bekdemir, *Ann Clin Microbiol Antimicrob* **2008**, *7*, 17-22.

[30] N. Ozbek, H. Katircioaylu, N. Karacan, T. Baykal, *Bioorg. Med. Chem.* **2007**, *15*, 5105-5109.

[31] E. D Clercq, *Curr. Med. Chem.* **2001**, *8*, 1543-1572.

[32] P. K. Naik, B. P. Chatterji, S. N. Vangapandu, R. Aneja, R. Chandra, S. Kanteveri, *J. Comput. Aided Mol. Des.* **2011**, *25*, 443–454.

[33] S. M. Kupchan, R. W. Britton, M. F. Ziegler, C. J. Gilmore, R. J. Restivo, R. F. Bryan, *J. Am. Chem. Soc.* **1973**, *95*, 1335–1336.

[34] G. D. Hatnapure, A. P. Keche, A. H. Rodge, S.S. Birajdar, R. H. Tale, V. M. Kamble, *Bioorg. Med. Chem. Lett.* **2012**, *22*, 6385-6390.

[35] a) N. K. Beyeh, A. Valkonen, K. Rissanen, *Org. Lett.* **2010**, *12*, 1392-1395; b) A. Kamal, P. S. M. M. Reddy, D. R. Reddy, E. Laxman, *Bioorg. Med. Chem.* **2006**, *14*, 385-394; c) C. S. A. Kumar, S. B. B. Prasad, K. Vinaya, S. Chandrappa, N. R. Thimmegowda, Y. C. S. Kumar, S. Swarup, K. S. Rangappa, *Eur.*

J. Med. Chem. **2009**, *44*, 1223-1229; d) C. S. A. Kumar, S. N. Swamy, N. R. Thimmegowda, S. B. B. Prasad, G. W. Yip, K. S. Rangappa, *Med. Chem. Res.* **2007**, *16*, 179-187.

[36] J. Z. Long, X. Jin, A. Adibekian, W. W. Li, B. F. Cravatt, *J. Med. Chem.* **2010**, *53*, 1830-1842.

[37] D. H. Jiang, M. Huang, *Chem. Reag.* **2012**, *34*, 797-799.

[38] S. Liang, C. M. Liu, Y. S. Jin, Q. Q. He, *J. Med. Chem.* **2004**, *14*, 71-75.

[39] Q. Wu, Z. C. Wang, X. Wei, W. Xue, *J. Synth. Chem.* **2014**, *22*, 429-434.

[40] R. J. Kerns, M. J. Rybak, G. W. Kaatz, F. Vaka, R. Cha, R. G. Grucz, V. U. Diwadkar, *Bioorg. Med. Chem. Lett.* **2003**, *13*, 2109–2112.

[41] C. Avijeet, A. Amy, G. Charles, *J. Biol. Chem.* **2014**, *289*, 2978–2991.

[42] a) R. Maia, C. Do, C. A. M. Fraga, *Curr. Enzyme Inhib.* **2010**, *6*,171−182; b) C. Lazar, A. Kluczyk, T. Kiyota, Y. Konishi, *J. Med. Chem.* **2004**, *47*, 6973−82.

[43] a) T. Mosmann, *J. Immunol. Meth.* **1983**, *65*, 55–63; b) P. Sharma, K. R. Senwar, M. K. Jeengar, T. S. Reddy, V. G. M. Naidu, A. Kamal, N. Shankaraiah, *Eur. J. Med. Chem.* **2015**, *104*, 11–24.

[44] a) P. Sharma, T. S. Reddy, D. Thummuri, K. R. Senwar, N. P. Kumar, V. Naidu, S. K. Bhargava, N. Shankaraiah, *Eur. J. Med. Chem.* **2016**, *124*, 608-621; b) R. Tokala, S. Thatikonda, S. Sana, P. Regur, C. Godugu, N. Shankaraiah, *New J. Chem.* **2018**, *42*, 16226–16236

[45] M. Yao, J. Yang, L. Cao, L. Zhang, S. Qu, H. Gao, *Mol. Med. Rep*. **2014**, *10*, 365-372.

[46] P. Sharma, D. Thummuri, T. S. Reddy, K. R. Senwar, V. G. M. Naidu, G. Srinivasulu, S. K. Bharghava, N. Shankaraiah, *Eur. J. Med. Chem.* **2016**, *122*, 584–600; b) K. R. Senwar, P. Sharma, T. S. Reddy, M. K. Jeengar, V. L. Nayak, V. G. M. Naidu, A. Kamal, N. Shankaraiah, *Eur. J. Med. Chem.* **2015**, *102*, 413–424.

[47] a) B. I. Tarnowski, F. G. Spinale, J. H. Nicholson, *Biotech Histochem*, **1991**, *66*, 297–302; b) R. Tokala, S. Thatikonda, U. S. Vanteddu, S. Sana, C. Godugu, N. Shankaraiah, *ChemMedChem*. **2018**, *13*, 1909–1922.

[48] a) N. Kulabas, E. Tatar, O. B. Ozakpinar, D. Ozsavci, C. Pannecouque, E. D. Clercq, I. Kucukguzel, *Eur. J. Med. Chem.* **2016**, *121*, 58–70; b) R. Tokala, S. Bale, I. P. Janrao, A. Vennela, N. P. Kumar, K. R. Senwar, C. Godugu, N. Shankaraiah, *Bioorg. Med. Chem. Lett.* **2018**, *28*, 1919–1924.

[49] U. V. Mallavadhani, C. V. Prasad, S. Shrivastava, V. Naidu, *Eur. J. Med. Chem.* **2014**, *83*, 84–91.

[50] a) V. Chaudhary, J. B Venghateri, H. P. S Dhaked, A. S Bhoyar, S. K Guchhait, D. Panda, *J. Med. Chem.* **2016**, *59,* 3439–3451; b) N. P. Kumar, S. Thatikonda, R. Tokala, S. S. Kumari, U. J. Lakshmi, C. Godugu, N. Shankaraiah, *Bioorg. Med. Chem.* **2018**, *26*, 1996–2008.

[51] N. Shankaraiah, S. Nekkanti, U. R. Brahma, N. P. Kumar, N. Deshpande, D. Prasanna, K. R. Senwar, U. J. Lakshmi, *Bioorg. Med. Chem.* **2017**, *25*, 4805–4816.

[52] R. Gaspari, A. E. Prota, K. Bargsten, A. Cavalli, M. O. Steinmetz, *Chem*, **2017**, *2*, 102–113.

[53] Schrödinger Suite **2017**-1, Schrödinger, LLC, New York, **2018**.

Insert graphic for Table of Contents here. ((Please ensure your graphic is in **one** of following formats))

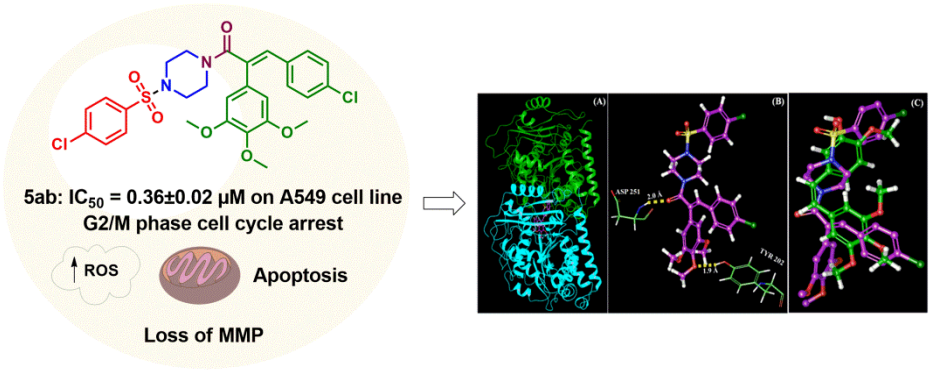

A series of CA4 linked sulfonyl piperazine derivatives *via* molecular hybridization were synthesized. The compound **5ab** was found as the active member by its *in vitro* cytotoxicity and exhibited potent tubulin polymerization inhibition.